Published in final edited form as:
Biochemistry. 2008 April 8; 47(14): 4306–4316.

DNA Tandem Lesion Repair by Strand Displacement Synthesis and Nucleotide Excision Repair†

Shuhei Imoto[‡,§], **Leslie A. Bransfield**[‡,§], **Deborah L. Croteau**[||], **Bennett Van Houten**[||], and **Marc M. Greenberg**[*,§]

Department of Chemistry, Johns Hopkins University, 3400 North Charles Street, Baltimore, Maryland 21218, and Laboratory of Molecular Genetics, National Institute of Environmental Health Sciences, National Institutes of Health, 111 T. W. Alexander Drive, Research Triangle Park, North Carolina 27709

Abstract

DNA tandem lesions are comprised of two contiguously damaged nucleotides. This subset of clustered lesions is produced by a variety of oxidizing agents, including ionizing radiation. Clustered lesions can inhibit base excision repair (BER). We report the effects of tandem lesions composed of a thymine glycol and a 5′-adjacent 2-deoxyribonolactone (LTg) or tetrahydrofuran abasic site (FTg). Some BER enzymes that act on the respective isolated lesions do not accept the tandem lesion as a substrate. For instance, endonuclease III (Nth) does not excise thymine glycol (Tg) when it is part of either tandem lesion. Similarly, endonuclease IV (Nfo) does not incise L or F when they are in tandem with Tg. Long-patch BER overcomes inhibition by the tandem lesion. DNA polymerase β (Pol β) carries out strand displacement synthesis, following APE1 incision of the abasic site. Pol β activity is enhanced by flap endonuclease (FEN1), which cleaves the resulting flap. The tandem lesion is also incised by the bacterial nucleotide excision repair system UvrABC with almost the same efficiency as an isolated Tg. These data reveal two solutions that DNA repair systems can use to counteract the formation of tandem lesions.

Isolated damaged nucleotides are believed to be the most common lesions resulting from DNA oxidation. As a result of efforts by many researchers, a great deal has been learned about how DNA lesions are repaired by base excision repair (BER)[1] and nucleotide excision repair (NER) (1–3). Recently, clusters of DNA lesions have been identified as significant components of radiation-induced damage. Clustered lesions consist of two or more damaged nucleotides within ~1.5 turns of duplex DNA and are attributed to multiple ionization events by a single radiation track. In principle, clustered lesions can contain modified nucleotides on a single strand, but biochemical studies have focused on bistranded lesions, which are possible progenitors to double strand breaks (1–11). Numerous studies have revealed the effects of clustered lesions on BER. The effects are dependent upon the nature of the lesions, as well as their proximity to one another in duplex DNA. Clustered lesions consisting of two contiguously damaged nucleotides are referred to as tandem lesions (12,13). Unlike other examples of clustered damage, tandem lesions can result from a single DNA damaging event, in which a

---

†We are grateful for support of this research by the National Institute of General Medical Science (Grant GM-063028). This research was supported in part by the Intramural Research Program of the NIH, National Institute of Environmental Health Sciences.

* To whom correspondence should be addressed. Tel: 410-516-8095. Fax: 410-516-7044. E-mail: mgreenberg@jhu.edu.
‡These researchers contributed equally to the research described in this paper.
§Johns Hopkins University.
||Laboratory of Molecular Genetics, NIEHS, NIH.

[1]Abbreviations: AP, abasic site; L, 2-deoxyribonolactone; F, tetrahydrofuran abasic site; Tg, thymine glycol; BER, base excision repair; LP-BER, long-patch base excision repair; NER, nucleotide excision repair; Nth, endonuclease III; Nfo, endonuclease IV; Xth, exonuclease III; APE1, apurinic/apyrimidinic endonuclease 1; Pol β, DNA polymerase β; FEN1, flap endonuclease 1.

reactive intermediate on one nucleotide reacts with an adjacent nucleotide. Hence, their formation is not limited to ionizing radiation and can be formed by a variety of reagents that produce the diffusible species hydroxyl radical. Studies on the repair of tandem lesions are more limited (14–16). Tandem lesions that contain a covalent link between the adjacent nucleobases are substrates for nucleotide excision repair (17,18). Herein we describe the repair of a tandem lesion (LTg) produced in DNA that is comprised of an oxidized abasic lesion previously shown to inhibit DNA repair and thymine glycol, as well as an analogue containing a tetrahydrofuran abasic site and thymine glycol (FTg) (Figure 1).

Tandem lesions are produced from nucleobase radicals, which are the major family of reactive species produced from the reaction of DNA with hydroxyl radical, or its direct ionization (12,19–23). Nucleobase reactive intermediates account for as much as 90% of the reactions between hydroxyl radical and DNA (24). Tandem lesions arise from reactions between nucleobase radicals and/or their respective peroxyl radicals with the 5′- or 3′-adjacent nucleotides (21,22,25–27). In studies on one pyrimidine radical, it was revealed that tandem lesions account for more than 80% of the modified DNA (25). The reactivity of the nucleobase peroxyl radicals is influenced by the helical twist of the DNA, which affects the accessibility of certain positions within the adjacent nucleotides. Consequently, a nucleobase peroxyl radical selectively abstracts the C1′-hydrogen atom of the 5′-adjacent nucleotide and also adds to the respective nucleobase. However, the peroxyl radical reacts only with the nucleobase of the 3′-adjacent nucleotide, because the hydrogen atoms (e.g., C1′-hydrogen atom) of the respective 2-deoxyribose are too far away. Abstraction of the 5′-adjacent nucleotide's C1′-hydrogen atom produces a tandem lesion containing 2-deoxyribonolactone (L) at the 5′-position that accounts for ~11% of the product pool (Scheme 1) (25). This mechanism for 2-deoxyribonolactone formation provides an explanation for recently reported observations that indicate that it is the major abasic lesion produced by γ-radiolysis and Fe-EDTA (which also produces hydroxyl radical), despite the fact that the C1′-hydrogen atom is inaccessible to diffusible species (28–30).

The tandem lesion containing 2-deoxyribonolactone is of particular interest because of the isolated oxidized abasic site's effects on replication and repair. 2-Deoxyribonolactone is an abasic lesion whose replication in *Escherichia coli* does not adhere to the A-rule (31,32). Instead, higher levels of 2′-deoxyguanosine, comparable to those of 2′-deoxyadenosine, are incorporated opposite the lesion (33). In addition, L presents an unusual challenge to BER. 2-Deoxyribonolactone is one of two DNA lesions known to form cross-links with repair proteins (34–36). The glycosylase endonuclease III (Nth), which repairs pyrimidine lesions such as thymine glycol (Tg), is a bifunctional enzyme that excises abasic sites (AP) via a lyase mechanism. Nth is cross-linked to L through the lysine side chain that it uses to form a Schiff base with its AP site target (36). In addition, L produces DNA–protein cross-links with DNA polymerase β (Pol β), following its incision by APE1 (37). In response, mammalian cells can circumvent the challenges posed by L by using long-patch BER (LP-BER) (38). In this study we show that incorporation of a modified nucleotide, thymine glycol (Tg), as part of a tandem lesion with 2-deoxyribonolactone (L) diminishes the ability of some BER enzymes to act on it, necessitating alternative pathways for its removal.

EXPERIMENTAL PROCEDURES

Materials and General Methods

Oligonucleotides were prepared on an Applied Biosystems Inc. 394 DNA synthesizer. The 50mer containing the fluoresceinylated thymidine was obtained from Sigma-Genosys. Commercially available DNA synthesis reagents, including the 5*R*,6*S*-thymine glycol phosphoramidite, were obtained from Glen Research Inc. Oligonucleotides containing the photolabile 2-deoxyribono-lactone precursor were synthesized as previously described (39).

Oligonucleotides containing Tg were synthesized using standard cycles as described by Iwai (40) and deprotected as described below. All others were synthesized and deprotected using standard protocols. Synthetic oligonucleotides containing Tg, L, and/or F were characterized by ESI-MS, which are included in the Supporting Information. DNA manipulations were carried out using standard procedures (41). T4 polynucleotide kinase, T4 DNA ligase, Xth, Nfo, APE1, and terminal deoxynucleotide transferase were obtained from New England Biolabs. FEN1 and Pol β were from Trevigen Inc. Plasmid containing the *nth* gene was obtained from Professor Yoke Wah Kow. Hexa-His-tagged Nth was isolated using the Novagen bugbuster kit and purified using a His • Bind column (Novagen). Its activity was determined as previously described (42). Radionuclides were obtained from Amersham Pharmacia. UvrABC was obtained as previously described (43,44). Analysis of radiolabeled oligonucleotides was carried out using a Storm 840 phosphorimager and ImageQuant 5.1 software. Kinetic constants were determined via nonlinear regression analysis of experimental data using Origin 6.1. The data presented in Tables 2 and 3are the average of two to five experiments (as noted below the tables). Each experiment consists of three replicates.

Deprotection Method for Oligonucleotides Containing Thymine Glycol (Tg)

The resin was suspended in ammonia at room temperature for 3 h. The resin was spun to the bottom, and the supernatant was transferred to another tube. The resin was washed with water (100 μL, 2×). The wash was combined with the supernatant and concentrated. The pellet was resuspended in 250 μL of a 1.4 M HF solution (1.5 mL of *N*-methylpyrrolidinone, 750 μL of TEA, 1.0 mL of TEA • HF) at 65 °C for 3 h. The solution was quenched with 3 M NaOAc (25 μL) and EtOH (1.0 mL), and the solution was kept at −80 °C for 1 h. The solution was spun at 13.2 rcf at 4 °C for 30 min. The supernatant was decanted and the pellet dried. The pellet was resuspended in 100 μL of formamide loading buffer (95% formamide, 10 mM EDTA) and loaded on a 20% denaturing PAGE gel (1.5 mm thick).

Kinetic Analysis of Thymine Glycol Excision by Nth

DNA solutions were prepared as 2× solutions of **1** ([DNA] = 1, 2, 6, 24, 50, 100, 200, 300 nM). A 2× enzyme solution was prepared containing 20 mM Hepes–KOH buffer (pH 7.4), 200 mM KCl, 20 mM EDTA, and 0.5 nM Nth. The 2× enzyme solution (5 μL) was added to the 2× DNA solution (5 μL) and allowed to react at 37 °C for 10 min and then quenched with 20 μL of formamide loading buffer (95% formamide, 10 mM EDTA). The quenched reactions were placed on ice. The solutions were denatured by heating at 90 °C for 90 s and immediately put on ice prior to loading on a 20% denaturing PAGE gel.

Time Course for Nth Excision of Thymine Glycol

A 2×DNA solution of **1** (100 nM) was prepared in a 1× buffer solution (20 μL) containing 10 mM Hepes–KOH buffer (pH 7.4), 100 mM KCl, and 10 mM EDTA. A 2× enzyme solution (0.5 nM, 20 μL) was prepared in the same 1× buffer solution. The enzyme solution (20 μL) was added to the DNA solution (20 μL) and incubated at 37 °C for 20 min. Aliquots (3 μL) were removed at 0.5, 1, 3, 5, 12, and 20 min and were quenched with 7 μL of formamide loading buffer (95% formamide, 10 mM EDTA).

The time course performed on the tandem lesions (3,4) was carried out in the same way as **1** except the 2× enzyme concentration was 200 nM, the 2× DNA solution was 2 nM, and aliquots were removed at 0, 10, 30, 60, 180, 300, 900, 1800, and 3600 s. The time course experiments for the clustered lesion containing duplexes (5,6) were run with a 2× DNA concentration of 2 nM and 2× enzyme concentration of 200 nM. Aliquots were removed at 0, 60, 180, 300, 900, 1800, and 3600 s.

Kinetic Analysis of 2-Deoxyribonolactone (L) Incision by Nfo

A 2× enzyme solution (5 μL) containing 10% glycerol, 20 mM Hepes–KOH (pH 7.4), 200 mM KCl, 200 mg/mL BSA, and 2 nM Nfo was added to 5 μL of a 2× DNA solution containing 20, 100, 200, 400, or 600 nM **2**. The solution was incubated at room temperature for 3.5 min before quenching with 20 μL of formamide loading buffer (95% formamide, 10 mM EDTA).

Time Course for Nfo Incision of 2-Deoxyribonolactone (L) or Tetrahydrofuran (F)

A 2× enzyme solution (10 μL) containing 10% glycerol, 20 mM Hepes–KOH (pH 7.4), 200 mM KCl, 200 mg/mL BSA, and 2 nM Nfo was added to 10 μL of a 2× DNA solution containing 25 nM **2**. The solution was incubated at room temperature for 30 min. Aliquots (1.5 μL) were removed at 0, 60, 180, 300, 900, and 1800 s and quenched with 10 μL of formamide loading buffer (95% formamide, 10 mM EDTA).

Experiments using the tandem lesion (3 or 4) were carried out in the same way as **2**, except a 2× enzyme concentration of 200 nM and a 2× DNA concentration of 2 nM were used. Aliquots (1.5 μL) were removed at 0, 10, 30, 60, 180, 300, 900, and 1800 s. Experiments using the clustered lesion containing duplexes (5,6) were carried out in the same way as **2** except aliquots (1.5 μL) were removed at 0, 10, 30, 60, 180, 300, 900, and 1800 s.

Kinetic Analysis of Xth Incision of 2-Deoxyribonolactone

A 2× enzyme solution (5 μL) containing 20 mM Bis-Tris-propane-HCl (pH 7.0), 20 mM $MgCl_2$, 2 mM dithiothreitol, and 25 pM Xth was added to 5 μL of a 2× DNA solution containing 10, 20, 50, 100, 150, or 200 nM **2**. The reaction was incubated at room temperature for 1 min and quenched with 20 μL of formamide loading buffer (95% formamide, 10 mM EDTA).

For experiments with the tandem lesion (3), 2× DNA concentrations used were 50, 100, 150, 250, 500, and 1000 nM, and the reaction time was 3 min. For experiments with the clustered lesion containing duplexes (5,6) the 2× DNA concentrations used were 20, 50, 100, 150, 250, and 400 nM, and the reaction time was 1 min.

Kinetic Analysis of APE1 Incision of 2-Deoxyribonolactone (L) or Tetrahydrofuran (F)

A 2× enzyme solution (5 μL) containing 100 mM potassium acetate, 40 mM Tris–acetate, 10 mM magnesium acetate, 1 mM dithiothreitol (pH 7.9), and 50 pM APE1 was added to 5 μL of a 2× DNA solution of **2** (10, 20, 50, 100, 150, or 250 nM). The solution was incubated at 37 °C for 2 min and quenched with 20 μL of formamide loading buffer (95% formamide, 10 mM EDTA).

Experiments with the tandem lesion (3,4) were carried out in the same way as **2** except using 2× DNA concentrations of 50, 100, 150, 250, 500, and 1000 nM. The experiments with the −1 and +1 cluster containing duplexes **5** and **6**, respectively, were carried out in the same way as **2** except 2× DNA concentrations used were 10, 20, 50, 100, 150, and 250 nM, and for the +1 cluster containing duplex **6**, the reaction time was 5 min instead of 2 min.

Nucleotide Excision Reaction by FEN1

3′-^{32}P-**4** (100 nM) was treated with APE1 (10 nM) at 37 °C for 15 min. FEN1 (25 nM) was then added to the resulting 3′-^{32}P-**8** (50 nM) and incubated in a buffer (30 μL) containing 50 mM Tris-HCl (pH = 7.5), 50 mM KCl, 0.2 mM EDTA, and 5 mM $MgCl_2$ at 37 °C for 1 h. Aliquots (2 μL) were removed at 1, 3, 5, 7, 15, 30, and 60 min and were quenched with 95% formamide loading buffer (8 μL). The reactions were analyzed by 20% denaturing PAGE.

Time Course of Pol β Extension of Tandem Lesion

Duplex 5′-^{32}P-labeled DNA–substrate (**4**, 100 nM) was treated with APE1 (10 nM) at 37 °C for 15 min. Pol β (5 nM) was then added to the resulting 5′-^{32}P-**8** (50 nM) in the absence or presence of FEN1 (25 nM) and incubated in a buffer containing 50 mM Tris-HCl (pH = 7.5), 50 mM KCl, 0.2mM EDTA, and 5 mM $MgCl_2$ at 37 °C for 1 h. Aliquots (2μL) were removed at 1, 3, 5, 7, 15, 30, and 60 min and were quenched with 95% formamide loading buffer (8 μL). The reactions were analyzed by 20% denaturing PAGE.

Cross-Linking of the LTg Tandem Lesion (7) with Pol β

Duplex 3′-labeled DNA–substrate (**1**, 100 nM) was treated with APE1 (10 nM) at 37 °C for 30 min. Pol β (500 nM) was then added to 3′-^{32}P-**7** (50 nM) and incubated in a buffer (30 μL) containing 50 mM Tris-HCl (pH = 7.5), 50 mM KCl, 0.2 mM EDTA, and 5 mM $MgCl_2$ at 37 °C for 24 h. Aliquots (2 μL) were removed at 0, 0.5, 1, 3, 9, and 24 h and were quenched with SDS loading buffer (8 μL). The reactions were loaded onto a 12% SDS–PAGE (0.4 mm thick), and the gel was run in TG buffer (25 mM Tris, 192 mM glycine, and 0.1% SDS) at 20 mA for 2.5 h.

Preparation of 9 and 10 by Enzyme Ligation

The 3′-terminal oligonucleotide (5 nmol) was treated with ATP (850 nmol) and T4 polynucleotide kinase (200 units) in kinase buffer (70 mM Tris-HCl, 10 mM $MgCl_2$, 5 mM dithiothreitol). The phosphorylation reaction was incubated at 37 °C for 1 h. The reaction mixture was lyophilized, then resuspended in water, and desalted using a G-25 Sephadex spin column. The phosphorylated 3′-side oligomer (5.0 nmol) was added to the 5′-side oligomer (7.5 nmol) and the appropriate template (7.5 nmol) in ligase buffer (50 mM Tris-HCl, 10 mM $MgCl_2$, 10 mM dithiothreitol, 1 mM ATP, 25 μg/mL BSA). The oligonucleotides were hybridized at 65 °C for 5 min and slowly cooled to 4 °C. After annealing, T4 DNA ligase (30000 units) was added, and the mixture was incubated at 16 °C for 1 h, followed by 3 h at 4 °C. The reaction was quenched by heating to 90 °C for 3 min and lyophilized, and the product was purified by 12% denaturing PAGE. The oligonucleotides used to construct **9** were 5′-d(AGC TAC GTA CGA GCT AG) and 5′-d(CTC GAC CFTg TAG GAC CTG CAG CTC CAG ATC TGT). The oligonucleotides used to construct **10** were 5′-d(AGC TAC GTA CGA GCT AGC TC) and 5′-d(GAC CTTg TAG GAC CTG CAG CTC CAG ATC TGT). In each instance, the template used was 5′-d(TGG AGC TGC AGG TCC TAA AGG TCG AGC TAG CTC GTA).

Time Course Analysis of UvrABC Incision

The DNA–substrates (**9**–**11**, 2 nM) were incubated with UvrA (20 nM), UvrB (100 nM), and UvrC (50 nM) in a 20 μL solution containing 50 mM Tris-HCl (pH = 7.5), 10 mM $MgCl_2$, 50 mM KCl, 1 mM ATP, and 5 mM dithiothreitol at 55 °C for 1 h. Just before the UvrABC solutions were added, the proteins were activated at 65 °C for 10 min, and UvrC was added last. Aliquots (2 μL) were removed at 0, 10, 30, 60, 180, 300, 900, 1800, and 3600 s and were quenched with formamide loading buffer (10 μL; 95% formamide, 10 mM EDTA).

RESULTS

Oligonucleotide Substrate Design and Synthesis

Tandemly damaged oligonucleotides for base excision repair (BER) experiments contained 2-deoxyribonolactone (L) or the tetrahydrofuran abasic site model (F) bonded through their 3′-phosphates to thymine glycol (Tg). Thymine glycol was chosen as the 3′-component of the tandem lesion because of its high *G*-value for radiation-induced formation (24). Moreover, Tg is formed via the same type of C6-peroxyl radical, which was independently shown to produce

tandem lesions containing L (25). Six 30-nucleotide long duplexes (1–6) were employed in BER experiments (Table 1). The sequences differed only at the positions where L (or F) and/or thymine glycol were (was) incorporated. Duplexes containing an isolated Tg or 2-deoxyribonolactone were studied in order to provide benchmarks for the results obtained with the tandem lesion substrate(s). Thymidine was substituted for either L or Tg in duplexes containing a single lesion. In addition, clustered lesions consisting of L and Tg on opposite strands were studied in order to compare to the tandem lesions. The same local sequences were incorporated into 16-nucleotide long duplexes (12–19) in order to probe the effects of the lesions on thermal stability.

Oligonucleotides containing Tg were prepared using a commercially available phosphoramidite originally described by Iwai (40). The Tg phosphoramidite consists of a single diastereomer (5*R*,6*S*). However, the 6-positions of 6-hydroxy-5,6-dihydropyrimidines epimerize in water following deprotection (45). Hence, the oligonucleotides containing Tg consist of a mixture of 5*R*,6*S* and 5*R*,6*R* stereoisomers. Duplexes containing L were prepared from the photolabile nitroindole derivative. Oligonucleotides containing the nitroindole were prepared as previously described (39). The 2-deoxyribonolactone was freshly prepared in duplex DNA via photolysis immediately before carrying out experiments. The extent of photoconversion was determined by treating an aliquot of the photolysate with NaOH (0.1 M, 37 °C) and was accounted for in all kinetic experiments.

Longer duplexes (50 nt) were constructed for nucleotide excision repair (NER) experiments in order to accommodate the UvrABC complex. A fluoresceinylated thymidine containing duplex was included as a control to compare to test the activity of the NER system (46). Duplexes containing thymine glycol or the FTg tandem lesion were prepared. The requisite 50-nt oligonucleotides containing FTg or Tg were prepared by ligating two shorter oligonucleotides on a 36-nt template. The yields of the oligonucleotides in **9** and **10** were 21% and 18%, respectively. The purity of the oligonucleotides was determined by enzymatic digestion (Supporting Information). The duplex containing Tg was treated with Nth, whereas the duplex containing the FTg tandem lesion was digested with APE1. In each instance 100% of the duplex was digested (see Supporting Information).

Nth Excision of Thymine Glycol (Tg)

Nth is a primary BER enzyme in *E. coli* responsible for excising Tg and a variety of other pyrimidine lesions. It is a bifunctional enzyme possessing glycosylase activity and a relatively robust lyase activity. The suitability of the 30mer duplexes as substrates for Nth was verified using DNA containing a single isolated Tg lesion (2). The kinetic parameters for excision ($K_m = 55.5 \pm 5.0$ nM, $k_{cat} = 8.2 \pm 1.9$ min^{-1}, $k_{cat}/K_m = 0.15 \pm 0.03$ nM^{-1} min^{-1}) are comparable to those reported in the literature (47). In contrast, attempts to carry out Tg excision when it is part of a tandem (3,4) or clustered lesion (5,6) under Michaelis–Menten conditions were unsuccessful. Little if any excision was detected. NaOH treatment of 3′-^{32}P-labeled substrates after incubation with Nth also failed to show any cleavage at the Tg lesion (data not shown). This indicated that the apparent lack of Nth activity was attributable to the tandem or clustered lesions' effects on the enzyme's glycosylase activity. In addition, cross-links were not observed between Nth and **3** even when the protein was present in large excess (data not shown). Evidence for binding of the clustered lesion was sought by questioning whether **3** inhibited excision of Tg from a duplex containing only this lesion (1). Addition of **3** (30 nM) to otherwise identical solutions as those used for determining Nth excision of Tg did not result in a diminution in the observed specificity constant, indicating that Tg in the tandem lesion is not strongly bound by the enzyme.

Reproducibly measurable amounts of Tg excision by Nth were only detectable when the lesion was a part of a clustered (5,6) or tandem lesion (3) when the enzyme was present in large (100-

fold) excess relative to substrate (Figure 2A). However, even then the amount of cleavage is modest and considerably smaller than that observed in DNA containing an isolated Tg lesion treated with a catalytic amount of enzyme. This behavior indicates that excision of Tg when part of a tandem or clustered lesion with 2-deoxyribonolac-tone is not limited by turnover. Comparable behavior was observed when Tg was flanked on the 5′-side by the tetrahydrofuran abasic site analogue (F, **4**) in which several percent of **4** was cleaved after 10 min in the presence of a 100-fold excess of Nth (Figure 2B). This observation indicates that the alkali-labile and chemically stable abasic lesions, L and F, respectively, affect Nth excision of Tg comparably.

Phosphodiesterase Incision of Abasic Sites

The first step in BER of abasic sites is incision by a 5′-phosphodiesterase. Nfo and Xth carry out this process in *E. coli*, with the latter being the primary enzyme responsible for this activity (48). These enzymes were reacted with the 30mer duplexes containing an isolated 2-deoxyribonolactone (2), as well as those containing tandem (3,4) or clustered lesions (5,6). Incision of L (2) by Nfo was carried out under Michaelis–Menten conditions. The kinetic constants [$K_m = 60.5 \pm 19.4$ nM, $k_{cat} = 2.4 \pm 0.5$ min^{-1}, $k_{cat}/K_m = (4.3 \pm 1.5) \times 10^{-2}$ nM^{-1} min^{-1}] determined for this reaction were comparable to those previously reported in a different sequence (49). However, Nfo incision of L that is part of a tandem (3) or clustered (5,6) lesion was extremely inefficient. A large excess (100-fold) of enzyme was required to induce measurable amounts of incision (Figure 3A). As was the case for Nth, a tandem lesion containing F adjacent to Tg (4) was also a poor substrate and required 100-fold equivalents of Nfo to produce significant levels of incision (Figure 3B). The amount of incision of the tandem and clustered lesions was comparable to that observed in the duplex containing isolated lactone (2) (Figure 3A). However, the concentration of Nfo was almost 10-fold less in the samples containing **2** than in those containing the tandem (3,4) or clustered lesions (5,6).

In contrast, Xth incises L when it is part of a tandem or clustered lesion with comparable efficiency compared to when the oxidized abasic site is part of an isolated lesion (Table 2). The specificity constant measured for incision of **2** containing L is ~35-fold greater than in the sequence previously reported (49). However, comparing the tandem lesion (3) to an isolated L (2) in an otherwise identical duplex indicates that the former is incised by Xth ~3-fold less efficiently and that the differences in the K_m's are the primary source of the disparate specificity constants (Table 2). The 2-deoxyribonolactone in the −1 (5) and +1 (6) clustered lesions is incised even more efficiently than the isolated lesion. In these substrates the higher specificity constant is attributable to a much greater k_{cat} (Table 2).

Incision by APE1 followed a similar pattern as Xth (Table 3). The duplex containing an isolated L (2) was incised ~5-fold more efficiently than in the sequence that was previously studied (50). The differences in the specificity constants between **2** and the previously reported substrate are primarily due to a lower K_m in the former. The tandem lesion containing L (3) is incised only slightly more poorly than when the oxidized abasic site is isolated in the duplex (2). The small difference is mostly attributable to an ~2-fold smaller k_{cat}. In addition, the duplex containing an FTg tandem lesion (4) is also a good substrate for APE1 (Table 3). The specificity constant for F incision in **4** is approximately one-half that for L when part of a tandem lesion with Tg in an otherwise identical duplex. Incision of clustered lesions containing L (5,6) is also efficient, although slower than in the duplex containing an isolated lesion.

Strand Displacement Synthesis and Cross-Linking by DNA Polymerase β (Pol β)

Although Nth is a prokaryotic BER enzyme, the observations made regarding its interactions with a LTg-containing duplex and those of APE1 led us to investigate tandem lesion repair by strand displacement synthesis in conjunction with FEN1. These experiments were carried out on the tandem lesion containing the stable tetrahydrofuran abasic site (F) because the DNA

containing a 2-deoxyribonolactone 5-phosphate terminus formed upon APE1 incision is chemically unstable. The facile elimination (data not shown) is consistent with the previously described behavior of DNA containing a 2-deoxyribose 5-phosphate at its 5′-terminus (51, 52). The similarity in the behavior of the FTg and LTg tandem lesions with respect to Nth, Xth, and APE1 activities suggested that the former would be a suitable model substrate of the respective lactone containing tandem lesion in strand displacement synthesis.

Utilizing the FTg-containing DNA in these experiments also obviates a potential competing process. Previous studies have shown that Pol β forms interstrand cross-links to L, following its incision by APE1 (37). This reaction is not possible when F is the substrate. Consequently, 3′-^{32}P-**3** was incised by APE1, and the resulting 3′-^{32}P-**7** was immediately reacted with Pol β in order to gauge whether DNA–protein cross-links were a viable pathway. Only modest amounts (1.2%) of cross-link were observed when Pol β was present in very high concentration (see Supporting Information). Moreover, the concentration of Pol β used in the cross-linking experiments was considerably higher than in the strand displacement experiments (see below). This indicated that cross-linking does not compete with strand displacement synthesis and substituting F for L in these experiments is acceptable.

Strand displacement synthesis substrate (5′-^{32}P-**8**), prepared from **4** (100 nM) under conditions ([APE1] = 10 nM, 15 min, 37 °C) that resulted in complete incision at the 5′-phosphate of F, was evident in subsequent experiments with DNA polymerase β (Pol β) and/or FEN1. Strand displacement synthesis by Pol β (5 nM) was examined in the absence or presence of FEN1 as a function of time (Figure 4). In the absence of FEN1 (Figure 4A,C) ~35% of the 5′-fragment in **8** was extended after 1 h. The majority of the strand displacement product was the result of the addition of two thymidine nucleotides. Elongation of the 5′-fragment was more rapid and more extensive in the presence of FEN1 (25 nM) (Figure 4B,C). The strand displacement synthesis product reached a plateau of ~70% and had a faster rise time than when FEN1 was absent (Figure 4C). In addition, almost 100% of the primer-extended product corresponded to 3-nucleotide addition (Figure 4B). These results were corroborated in experiments using 3′-^{32}P-**8** (Figure 5). Three nucleotides were excised in the presence of Pol β and FEN1 (Figure 5A). There was no evidence of any intermediate excision product, indicating that FEN1 cleaved a 3-nucleotide flap exclusively. In addition, excision in 3′-^{32}P-**8** was not observed in the absence of FEN1 or Pol β. The aggregate of these results reveals that FEN1 is solely responsible for cleaving the tandem lesion, but its ability to do so is dependent on the creation of a flap resulting from Pol β-mediated strand displacement synthesis.

Nucleotide Excision Repair of a Tandem Lesion

As an alternative to the type of long-patch BER pathway observed above, we investigated whether a tandem lesion was a substrate for nucleotide excision repair. The bacterial UvrABC NER system from *Bacillus caldotenax* was utilized (53). Because the optimal operating temperature for this system is 55 °C, and L is thermally unstable, the FTg tandem lesion (9) was employed. The excision efficiency of the tandem lesion was compared to an isolated thymine glycol (10), as well as a duplex containing a 5-fluoresceinylated thymidine (11) (46, 54). The latter was previously characterized using this system and served as a standard for comparison. The tandem lesion was a slightly poorer substrate than the duplex containing an isolated Tg. After 15 min, 32.2 ± 1.4% of the duplex containing FTg was incised, whereas 41.3 ± 2.2% of the thymine glycol containing substrate was cleaved. This differential was maintained throughout the course of the reaction. For instance, 71.1 ± 3.0% of the Tg substrate was incised after 60 min, during which only 56.9 ± 5.4% of the tandem lesion was cleaved. Either duplex was cleaved 2–3-fold more slowly than the standard duplex containing fluoresceinylated thymidine (Figure 6A). The positions at which incision occurred in the Tg- and FTg-containing duplexes were determined using the 5′-^{32}P- and 3′-^{32}P-labeled duplexes.

In each instance incision on the 5′-side of the lesion occurred seven nucleotides upstream from the lesion (Figure 6B). 3′-Incision of the tandem lesion (9) occurred three nucleotides downstream, whereas two incision sites three and four nucleotides downstream from Tg (10) were observed in the duplex containing the isolated lesion (Figure 6C).

UV Melting Temperatures of Modified DNA

Isolated lesions such as L and Tg are known to reduce duplex thermal stability (55,56). In the sequence context studied here each lesion lowered the T_m of a 16-nucleotide duplex 10–11 ° C (Table 4). Interestingly, the presence of the tandem lesion did not reduce the T_m any further. The lack of an effect on the T_m of adding a second lesion was unique to the tandem lesion, as the T_m's of the clustered lesions were reduced relative to those of the duplexes containing either isolated lesion. Examination of duplexes containing L and a mismatch (C) opposite either a 3′-adjacent T or Tg exhibits reduced T_m's relative to those containing an opposing A. This indicates that the thymine and thymine glycol form Watson–Crick base pairs with the opposing nucleotide. The lack of a difference in the T_m's between the tandem lesion and duplexes containing isolated lesions may indicate that little or no additional structural perturbation is introduced when the second lesion is incorporated. One could imagine that when Tg is substituted for T in a duplex containing L, the greater steric requirements of the nonplanar dihydropyrimidine (Tg) are readily accommodated due to the free space created by the abasic site. The bulk of the penalty for loss of π-stacking and hydrogen bonding was paid when the 2-deoxyribonolactone was introduced. The dihydropyrimidine ring's substituents occupy some of the space left vacant by loss of the nucleobase, reducing the disruption in base stacking typically introduced when Tg is incorporated in a normal duplex. Similarly, we speculate that the disruption in base stacking resulting from substituting Tg for T is partially alleviated when L replaces the 5′-adjacent thymidine. This partially compensates for the loss of the heterocyclic base resulting in the observed no net change in T_m. The ultimate outcome of these substitutions is that there is little difference in the melting temperatures of duplexes containing LTg or either isolated lesion. The hypothesis that tandem abasic and thymine glycol lesions help to offset each other's duplex destabilization is consistent with the effects of clustered lesions (17,18) on duplex T_m's. The T_m's of **17** and **18** in which the abasic site is not in a position to alleviate the disruption in base stacking by Tg's dihydropyrimidine ring are lower than those of the comparable duplexes containing isolated lesions.

DISCUSSION

Base excision repair enzymes that excise isolated damaged nucleotides are inhibited when the modifications are part of bistranded clustered lesions. The degree of inhibition depends upon the proximity of the lesions to one another. Inhibiting BER of bistranded lesions prevents the potential formation of double strand breaks. Tandem lesions are not potential sources of double strand breaks. Nonetheless, they can affect BER (14–16). The most common type of pyrimidine nucleobase radical generated by γ-radiolysis produces the tandem lesion containing 2-deoxyribonolactone adjacent to thymine glycol (LTg). On the basis of the interaction of the isolated individual modifications with repair enzymes, we anticipated that the LTg tandem lesion would present a dilemma to Nth. Thymine glycol is readily excised by Nth, but 2-deoxyribonolactone cross-links this enzyme (35,36). The outcome of combining Tg and L into a tandem lesion was that Nth excised Tg extremely inefficiently and L did not trap the enzyme.

Even if Tg in the tandem lesion was a substrate for Nth, 2-deoxyribonolactone would need to be removed by a different enzyme, because of its known cross-linking to lyases. Endonuclease incision of L, which is the first step in the primary pathway for AP site repair, was a likely alternative. Xth and APE1 are the enzymes principally responsible for the first step in AP lesion repair in *E. coli* and mammalian cells, respectively (48). In *E. coli*, a second enzyme, Nfo,

accounts for ~10% of the total AP endonuclease activity. Although isolated L is a substrate for Nfo, Xth, and APE1, incision of L by Nfo is inefficient when part of the LTg (or FTg) tandem lesion (49,50). In contrast, Xth and APE1 efficiently incise the tandem lesions (LTg, FTg). Although the source of the differences in interactions of the tandem lesions with Nfo versus Xth and APE1 is uncertain, possible explanations were considered. For instance, it is interesting to note that Xth and APE1 share a common structural motif and magnesium-dependent mechanism, while Nfo utilizes zinc to activate water toward nucleophilic attack on phosphate (48). Thermodynamics were considered as a source for what makes the tandem lesion a poorer substrate than DNA containing an isolated 2-deoxyribonolactone. Nfo, Xth, and APE1 are flippases. Hence, one might expect there to be an inverse correlation between duplex thermal stability and enzyme activity. However, T_m measurements indicate that duplexes containing the tandem lesion and isolated 2-deoxyribonolactone (or thymine glycol) are destabilized to a comparable extent. Diminution of Nfo binding to the LTg tandem lesion relative to DNA containing the lactone also does not explain inefficient incision. The apparent binding of Nfo, as determined by nondenaturing electrophoresis, is ~3-fold weaker for the tandem lesion than for isolated 2-deoxyribonolactone (data not shown).

Single nucleotide excision of an abasic site analogue (F) by APE1 and Pol β is coordinated (57). However, the combination of efficient incision of L (or F) by Xth and APE1, Nth's inability to excise Tg in a tandem lesion, and previous knowledge that Pol β does not excise L led us to investigate the viability of long-patch BER (LP-BER) (37). Strand displacement synthesis by Pol β in the presence or absence of FEN1 was examined using a tandem lesion substrate containing tetrahydrofuran (F) in place of L. 5′-Deoxyribose phosphate generated by incision of an AP lesion rapidly undergoes elimination during gel electrophoresis. Consequently, incised AP sites are reduced prior to electrophoresis analysis in order to correctly interpret kinetic experiments (51,52). This treatment cannot be utilized in studies on incised L because the lactone is not reduced by sodium borohydride. Substituting F for L prevents the spontaneous elimination of the 5′-phosphorylated lactone. Furthermore, kinetic studies showed that Nth and APE1 treated LTg and FTg tandem lesions comparably (Table 3,Figure 2), indicating that the chemically stable tandem lesion would be a suitable model for LP-BER of the true lesion. Analysis of 5′- and 3′-^{32}P-labeled substrates revealed Pol β and FEN1 activities, respectively. The substrate was designed to contain three consecutive 2′-deoxyadenosines in the opposing strand such that the presence of a single nucleotide triphosphate (dTTP) would give rise to a maximum incorporation of three nucleotides. Indeed, three nucleotides were incorporated in the oligonucleotide flanking the incised tandem lesion strand in the presence of Pol β and FEN1. The incorporation of these nucleotides coincided with cleavage of three nucleotides from the 5′-terminus of the incised oligonucleotide containing the tandem lesion. Products resulting from cleavage of one or two nucleotides by FEN1 were not detected. In the absence of FEN1 mostly two nucleotides were incorporated, and the rate at which the strand was extended was slower than in the presence of FEN1. Buildup of single nucleotide extension product was not observed, regardless of whether FEN1 was present, indicating that addition of the first two nucleotides is faster than the third. Although some of the third nucleotide is incorporated in the absence of FEN1, it is not possible to determine from these data whether the third nucleotide is only added before cleavage of the three-nucleotide flap (Figure 7). These observations are consistent with reports in which FEN1 was shown to stimulate strand displacement synthesis repair of nicked DNA by Pol β (58–60). However, there is a difference in the synergism between Pol β and FEN1 operating on the tandem lesion compared to a nicked substrate containing F at the incision point (60). In contrast to nicked DNA repair where FEN1 activity was comparable in the absence or presence of Pol β, FEN1 does not act on the tandem lesion at all in the absence of the polymerase.

These data indicate that LP-BER overcomes the inhibition of some repair proteins. However, it is not unusual for an organism to employ redundant DNA repair pathways to protect its

genome (61–63). Consequently, we examined repair of the FTg tandem lesion by the UvrABC system. Bacterial NER systems recognize thymine glycol, but not dihydrothymine (54,64). Presumably, this is because the latter induces a modest perturbation in the duplex structure by adopting a conformation in which the methyl group occupies a pseudoequatorial orientation (65). Thymine glycol exerts a more significant perturbation to base stacking because it cannot avoid having one of the non-hydrogen atom substituents on carbons 5 and 6 occupy a pseudoaxial orientation. Although the lesions were not compared to one another in similar substrates side by side, Tg is not as high in the NER hierarchy of substrates as strongly helix distorting lesions, such as *cis*-platin G-G intrastrand cross-links (66). The incorporation of Tg into a tandem lesion adjacent to an abasic site resulted in a modest (20%) reduction in nucleotide excision repair activity compared to an isolated thymine glycol after 15 and 60 min of reaction. We hypothesize that this is due to a smaller distortion of the helix by the tandem lesion than an isolated Tg because the space created by loss of the adjacent nucleobase can be used to accommodate a pseudoaxial substituent. This explanation is consistent with the T_m studies (Table 4), which showed that the tandem lesion containing duplex and those containing isolated L or Tg lesions were of comparable thermal stability.

Summary

We have shown that a unique tandem lesion that is produced in DNA as a result of oxidative stress requires adaptation by the DNA repair system in vitro. The presence of a 2-deoxyribonolactone (L) at the 5′-adjacent position of thymine glycol (Tg) prevents Nth from excising the modified pyrimidine nucleotide. Similarly, L incision by Nfo is also hindered by the proximity of Tg, but the activities of other phosphodiesterases (APE1, Xth) that are mechanistically distinct from Nfo are unaffected. The BER system overcomes the challenge presented by the tandem lesion by employing a LP-BER approach in which Pol β and FEN1 work together to remove the damaged DNA. LP-BER of the tandem lesion is distinguishable from that of isolated abasic lesions if the FEN1 is inactive in the absence of Pol β. However, as is the case with other reported lesions, fill-in by Pol β is stimulated by FEN1. This investigation also reveals that redundancies in the DNA repair system will enable an organism to protect the genome against the LTg tandem lesion by excising the lesion via the NER pathway. Incision of a closely related model tandem lesion (FTg) is only slightly less efficient than that of an isolated Tg. Although the LTg tandem lesion has not yet been characterized in vivo, these studies reveal two potential pathways for its repair. The tandem lesion effects on replication also have not yet been reported. However, these studies suggest that such investigations are warranted.

Supplementary Material

Refer to Web version on PubMed Central for supplementary material.

Acknowledgements

We thank Professor Yoke Wah Kow for providing the plasmid used for expressing Nth.

References

1. Ho ELY, Parent M, Satoh MS. Induction of Base Damages Representing a High Risk Site for Double-strand DNA Break Formation in Genomic DNA by Exposure of Cells to DNA Damaging Agents. J Biol Chem 2007;282:21913–21923. [PubMed: 17545165]
2. Hada M, Sutherland BM. Spectrum of complex DNA damages depends on the incident radiation. Radiat Res 2006;165:223–230. [PubMed: 16435920]
3. Shikazono N, Pearson C, O'Neill P, Thacker J. The Roles of Specific Glycosylases in Determining the Mutagenic Consequences of Clustered DNA Base Damage. Nucleic Acids Res 2006;34:3722–3730. [PubMed: 16893955]

4. Budworth H, Matthewman G, O'Neill P, Dianov GL. Repair of Tandem Base Lesions in DNA by Human Cell Extracts Generates Persisting Single-strand Breaks. J Mol Biol 2005;351:1020–1029. [PubMed: 16054643]
5. Lomax ME, Cunniffe S, O'Neill P. Efficiency of Repair of an Abasic Site within DNA Clustered Damage Sites by Mammalian Cell Nuclear Extracts. Biochemistry 2004;43:11017–11026. [PubMed: 15323560]
6. Chaudhry MA, Weinfeld M. Reactivity of human apurinic/apyrimidinic endonuclease and *Escherichia coli* exonuclease III with bistranded abasic sites in DNA. J Biol Chem 1997;272:15650–15655. [PubMed: 9188454]
7. Harrison L, Brame KL, Geltz LE, Landry AM. Closely opposed apurinic/apyrimidinic sites are converted to double strand breaks in *Escherichia coli* even in the absence of exonuclease III, endonuclease IV, nucleotide excision repair and AP lyase cleavage. DNA Repair 2006;5:324–335. [PubMed: 16337438]
8. Malyarchuk S, Brame KL, Youngblood R, Shi R, Harrison L. Two clustered 8-oxo-7,8-dihydroguanine (8-oxodG) lesions increase the point mutation frequency of 8-oxodG, but do not result in double strand breaks or deletions in *Escherichia coli*. Nucleic Acids Res 2004;32:5721–5731. [PubMed: 15509868]
9. Weinfeld M, ResouliNia A, Chaudhry MA, Britten RA. Response of Base Excision Repair Enzymes to Complex DNA Lesions. Radiat Res 2001;156:584–589. [PubMed: 11604076]
10. Blaisdell JO, Wallace SS. Abortive base-excision repair of radiation-induced clustered DNA lesions in *Escherichia coli*. Proc Natl Acad Sci USA 2001;98:7426–7430. [PubMed: 11404468]
11. Harrison L, Hatahet Z, Wallace SS. *In Vitro* Repair of Synthetic Ionizing Radiation-induced Multiply Damaged DNA Sites. J Mol Biol 1999;290:667–684. [PubMed: 10395822]
12. Box HC, Patrzyc HB, Dawidzik JB, Wallace JC, Freund HG, Iijima H, Budzinski EE. Double base lesions in DNA X-irradiated in the presence or absence of oxygen. Radiat Res 2000;153:442–446. [PubMed: 10761005]
13. Box HC, Wallace JC. Free Radical-Induced Double Base Lesions. Radiat Res 1995;141:91. [PubMed: 7997520]
14. Ali MM, Hazra TK, Hong D, Kow YW. Action of Human Endonucleases III and VIII Upon DNA-containing Tandem Dihydrouracil. DNA Repair 2005;4:679–686. [PubMed: 15907775]
15. Venkhataraman R, Donald CD, Roy R, You HJ, Doetsch PW, Kow YW. Enzymatic Processing of DNA Containing Tandem Dihydrouracil by Endonucleases III and VIII. Nucleic Acids Res 2001;29:407–414. [PubMed: 11139610]
16. Bourdat AG, Gasparutto D, Cadet J. Synthesis and enzymatic processing of oligodeoxynucleotides containing tandem base damage. Nucleic Acids Res 1999;27:1015–1024. [PubMed: 9927734]
17. Gu C, Zhang Q, Yang Z, Wang Y, Zou Y, Wang Y. Recognition and Incision of Oxidative Intrastrand Cross-Link Lesions by UvrABC Nuclease. Biochemistry 2006;45:10739–10746. [PubMed: 16939226]
18. Yang Z, Colis LC, Basu AK, Zou Y. Recognition and incision of gamma-radiation-induced cross-linked guanine-thymine tandem lesion G[8,5-Me]T by UvrABC nuclease. Chem Res Toxicol 2005;18:1339–1346. [PubMed: 16167825]
19. Bourdat AG, Douki T, Frelon S, Gasparutto D, Cadet J. Tandem Base Lesions Are Generated by Hydroxyl Radical within Isolated DNA in Aerated Aqueous Solution. J Am Chem Soc 2000;122:4549–4556.
20. Douki T, Riviere J, Cadet J. DNA Tandem Lesions Containing 8-Oxo-7,8-dihydroguanine and Formamido Residues Arise from Intramolecular Addition of Thymine Peroxyl Radical to Guanine. Chem Res Toxicol 2002;15:445–454. [PubMed: 11896694]
21. Zhang Q, Wang Y. Generation of 5-(2′-deoxycyti-dyl)methyl radical and the formation of intrastrand cross-link lesions in oligodeoxyribonucleotides. Nucleic Acids Res 2005;33:1593–1603. [PubMed: 15767284]
22. Hong H, Cao H, Wang Y. Identification and Quantification of a Guanine-Thymine Intrastrand Cross-Link Lesion Induced by Cu(II)/H202/Ascorbate. Chem Res Toxicol 2006;19:614–621. [PubMed: 16696563]
23. Greenberg MM. Elucidating DNA Damage and Repair Processes by Independently Generating Reactive and Metastable Intermediates. Org Biomol Chem 2007;5:18–30. [PubMed: 17164902]

24. von Sonntag, C. Free-Radical-Induced DNA Damage and Its Repair. Springer-Verlag; Berlin: 2006.
25. Hong IS, Carter KN, Sato K, Greenberg MM. Characterization and Mechanism of Formation of Tandem Lesions in DNA by a Nucleobase Peroxyl Radical. J Am Chem Soc 2007;129:4089–4098. [PubMed: 17335214]
26. Romieu A, Bellon S, Gasparutto D, Cadet J. Synthesis and UV Photolysis of Oligodeoxynucleotides That Contain 5-(Phenylthiomethyl)-2′-deoxyuridine: A Specific Photolabile Precursor of 5-(2′-Deoxyuridilyl)methyl Radical. Org Lett 2000;2:1085–1088. [PubMed: 10804560]
27. Carter KN, Greenberg MM. Tandem Lesions are the Major Products Resulting from a Pyrimidine Nucleobase Radical. J Am Chem Soc 2003;125:13376–13378. [PubMed: 14583031]
28. Roginskaya M, Razskazovskiy Y, Bernhard WA. 2-Deoxyribonolactone Lesions in X-ray-Irradiated DNA: Quantitative Determination by Catalytic 5-Methylene-2-furanone Release. Angew Chem, Int Ed 2005;44:6210–6213.
29. Roginskaya M, Bernhard WA, Marion RT, Razskazovskiy Y. The Release of 5-Methylene-2-Furanone from Irradiated DNA Catalyzed by Cationic Polyamines and Divalent Metal Cations. Radiat Res 2005;163:85–89. [PubMed: 15606311]
30. Xue L, Greenberg MM. Use of Fluorescence Sensors to Determine that 2-Deoxyribonolactone is the Major Alkali-Labile Deoxyribose Lesion Produced in Oxidatively Damaged DNA. Angew Chem, Int Ed 2007;46:561–564.
31. Strauss BS. Getting Around. DNA Repair 2005;4:951–957. [PubMed: 16023062]
32. Strauss BS. The “A Rule” of Mutagen Specificity: a Consequence of DNA Polymerase Bypass of Non-Instructional Lesions? BioEssays 1991;13:79–84. [PubMed: 2029269]
33. Kroeger KM, Jiang YL, Kow YW, Goodman MF, Greenberg MM. Mutagenic Effects of 2-Deoxyribono-lactone in *Escherichia coli*. An Abasic Lesion That Disobeys the A-Rule. Biochemistry 2004;43:6723–6733. [PubMed: 15157106]
34. Makino K, Ide H. DNA-Protein Cross-link Formation Mediated by Oxanine. A Novel Genotoxic Mechanism of Nitric Oxide-induced DNA Damage. J Biol Chem 2003;278:25264–25272. [PubMed: 12719419]
35. Kroeger KM, Hashimoto M, Kow YW, Greenberg MM. Cross-Linking of 2-Deoxyribonolactone and Its β-Elimination Product by Base Excision Repair Enzymes. Biochemistry 2003;42:2449–2455. [PubMed: 12600212]
36. Hashimoto M, Greenberg MM, Kow YW, Hwang JT, Cunningham RP. The 2-Deoxyribonolactone Lesion Produced in DNA by Neocarzinostatin and Other DNA Damaging Agents Forms Cross-links with the Base-Excision Repair Enzyme Endonuclease III. J Am Chem Soc 2001;123:3161–3162. [PubMed: 11457038]
37. DeMott MS, Beyret E, Wong D, Bales BC, Hwang JT, Greenberg MM, Demple B. Covalent Trapping of Human DNA Polymerase β by the Oxidative DNA Lesion 2-Deoxyribonolactone. J Biol Chem 2002;277:7637–7640. [PubMed: 11805079]
38. Sung JS, Demott MS, Demple B. Long-patch base excision DNA repair of 2-deoxyribonolactone prevents the formation of DNA-protein cross-links with DNA polymerase β. J Biol Chem 2005;280:39095–39103. [PubMed: 16188889]
39. Kotera M, Roupioz Y, Defrancq E, Bourdat AG, Garcia J, Coulombeau C, Lhomme J. The 7-nitroindole nucleoside as a photochemical precursor of 2′-deoxyribonolactone: access to DNA fragments containing this oxidative abasic lesion. Chem Eur J 2000;6:4163–4169.
40. Iwai S. Synthesis and Thermodynamic Studies of Oligo-nucleotides Containing the Two Isomers of Thymine Glycol. Chem Eur J 2001;7:4343–4351.
41. Maniatis, T.; Fritsch, EF.; Sambrook, J. Molecular Cloning. Cold Spring Harbor Laboratory; Cold Spring Harbor, NY: 1982.
42. Ikeda S, Biswa T, Ro R, Izumi T, Boldog I, Kurosky A, Sarkei AH, Seki S, Mitra S. Purification and Characterization of Human NTH1, a Homolog of *Escherichia coli* Endonuclease III. J Biol Chem 1998;273:21585–21593. [PubMed: 9705289]
43. Wang H, DellaVecchia MJ, Skorvaga M, Croteau DL, Erie DA, Van Houten B. UvrB domain 4, an autoinhibitory gate for regulation of DNA binding and ATPase activity. J Biol Chem 2006;281:15227–15237. [PubMed: 16595666]

44. Croteau DL, DellaVecchia MJ, Wang H, Bienstock RJ, Melton MA, Van Houten B. The C-terminal zinc finger of UvrA does not bind DNA directly but regulates damage-specific DNA binding. J Biol Chem 2006;281:26370–26381. [PubMed: 16829526]
45. Carter KN, Greenberg MM. Direct Measurement of Pyrimidine C6-hydrate Stability. Bioorg Med Chem 2001;9:2341–2346. [PubMed: 11553474]
46. Skorvaga M, Theis K, Mandavilli BS, Kisker C, Van Houten B. The β-Hairpin Motif of UvrB is Essential for DNA Binding, Damage Processing, and UvrC-mediated Incisions. J Biol Chem 2002;277:1553–1559. [PubMed: 11687584]
47. Asagoshi K, Odawara H, Nakano H, Miyano T, Terato H, Ohyama Y, Seki S, Ide H. Comparison of Substrate Specificities of *Escherichia coli* Endonuclease III and Its Mouse Homologue (mNTH1) Using Defined Oligonucleotide Substrates. Biochemistry 2000;39:11389–11398. [PubMed: 10985784]
48. Friedberg, EC.; Walker, GC.; Siede, W.; Wood, RD.; Schultz, RA.; Ellenberger, T. DNA Repair and Mutagenesis. 2. ASM Press; Washington, DC: 2006.
49. Greenberg MM, Weledji YN, Kim J, Bales BC. Repair of Oxidized Abasic Sites by Exonuclease III, Endonuclease IV, and Endonuclease III. Biochemistry 2004;43:8178–8183. [PubMed: 15209514]
50. Xu, Y-j; De Mottt, MS.; Hwang, JT.; Greenberg, MM.; Demple, B. Action of Human Apurinic Endonuclease (Ape1) on C1′-Oxidized Deoxyribose Damage in DNA. DNA Repair 2003;2:175–185. [PubMed: 12531388]
51. Sobol RW, Prasad R, Evenski A, Baker A, Yang XP, Horton JK, Wilson SH. The lyase activity of the DNA repair protein beta-polymerase protects from DNA-damage-induced cytotoxicity. Nature 2000;405:807–810. [PubMed: 10866204]
52. Matsumoto Y, Kim K. Excision of Deoxyribose Phosphate Residues by DNA Polymerase Beta During DNA Repair. Science 1995;269:699–702. [PubMed: 7624801]
53. Van Houten B, Croteau DL, DellaVecchia MJ, Wang H, Kisker C. Close-fitting sleeves": DNA damage recognition by the UvrABC nuclease system. Mutat Res 2005;577:92–117. [PubMed: 15927210]
54. Kow YW, Wallace SS, Van Houten B. UvrABC Nuclease Complex Repairs Thymine Glycol, an Oxidative DNA Base Damage. Mutat Res 1990;235:147–156. [PubMed: 2407949]
55. Roupioz Y, Lhomme J, Kotera M. Chemistry of the 2-Deoxyribonolactone Lesion in Oligonucleotides: Cleavage Kinetics and Products Analysis. J Am Chem Soc 2002;124:9129–9135. [PubMed: 12149017]
56. Iwai S. Synthesis and Thermodynamic Studies of Oligo-nucleotides Containing the Two Isomers of Thymine Glycol. Chem Eur J 2001;7:4343–4351.
57. Liu Y, Prasad R, Beard WA, Kedar PS, Hou EW, Shock DD, Wilson SH. Coordination of Steps in Single-nucleotide Base Excision Repair Mediated by Apurinic/Apyrimidinic Endonuclease 1 and DNA Polymerase β. J Biol Chem 2007;282:13532–13541. [PubMed: 17355977]
58. Prasad R, Dianov GL, Bohr VA, Wilson SH. FEN1 Stimulation of DNA Polymerase beta Mediates an Excision Step in Mammalian Long Patch Base Excision Repair. J Biol Chem 2000;275:4460–4466. [PubMed: 10660619]
59. Prasad R, Lavrik OI, Kim SJ, Kedar P, Yang XP, Vande Berg BJ, Wilson SH. DNA Polymerase beta-mediated Long Patch Base Excision Repair. Poly(ADP-Ribose) Polymerase-1 Stimulates Strand Displacement DNA Synthesis. J Biol Chem 2001;276:32411–32414. [PubMed: 11440997]
60. Liu Y, Beard WA, Shock DD, Prasad R, Hou EW, Wilson SH. DNA polymerase beta and flap endonuclease 1 enzymatic specificities sustain DNA synthesis for long patch base excision repair. J Biol Chem 2005;280:3665–3674. [PubMed: 15561706]
61. Ho E, Satoh MS. Repair of Single-Strand DNA Interruptions by Redundant Pathways and Its Implication in Cellular Sensitivity to DNA-damaging Agents. Nucleic Acids Res 2003;31:7032–7040. [PubMed: 14627836]
62. Parsons JL, Elder RH. DNA N-glycosylase deficient mice: a tale of redundancy. Mutat Res 2003;531:165–175. [PubMed: 14637253]
63. Ishchenko AA, Deprez E, Maksimenko A, Brochon JC, Tauc P, Saparbaev MK. Uncoupling of the Base Excision and Nucleotide Incision Repair Pathways Reveals Their Respective Biological Roles. Proc Natl Acad Sci USA 2006;103:2564–2569. [PubMed: 16473948]

64. Lin JJ, Sancar A. A new mechanism for repairing oxidative damage to DNA: (A)BC exonuclease removes AP sites and thymine glycols from DNA. Biochemistry 1989;28:7979–7984. [PubMed: 2690930]

65. Miaskiewicz K, Miller J, Osman R. Energetic basis for structural preferences in 5/6-hydroxy-5,6-dihydropyrimidines: products of ionizing and ultraviolet radiation action on DNA bases. Biochim Biophys Acta 1994;1218:283–291. [PubMed: 8049253]

66. Reardon JT, Sancar A. Nucleotide Excision Repair. Prog Nucleic Acid Res Mol Biol 2005;79:183–235. [PubMed: 16096029]

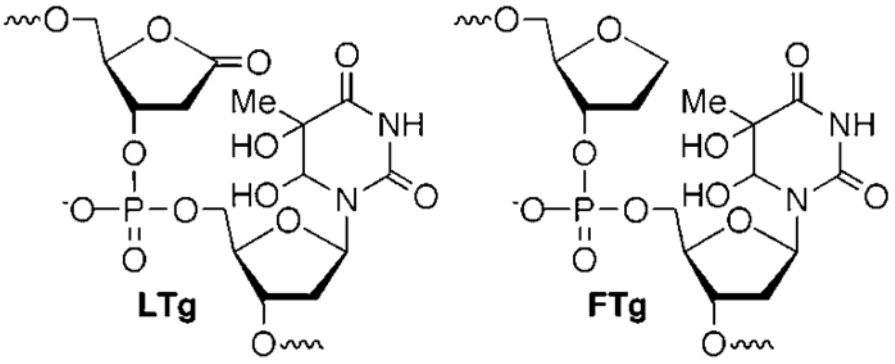

Figure 1.
Chemical structures of the tandem lesions. These constructs were incorporated in the corresponding duplexes that are listed in Table 1.

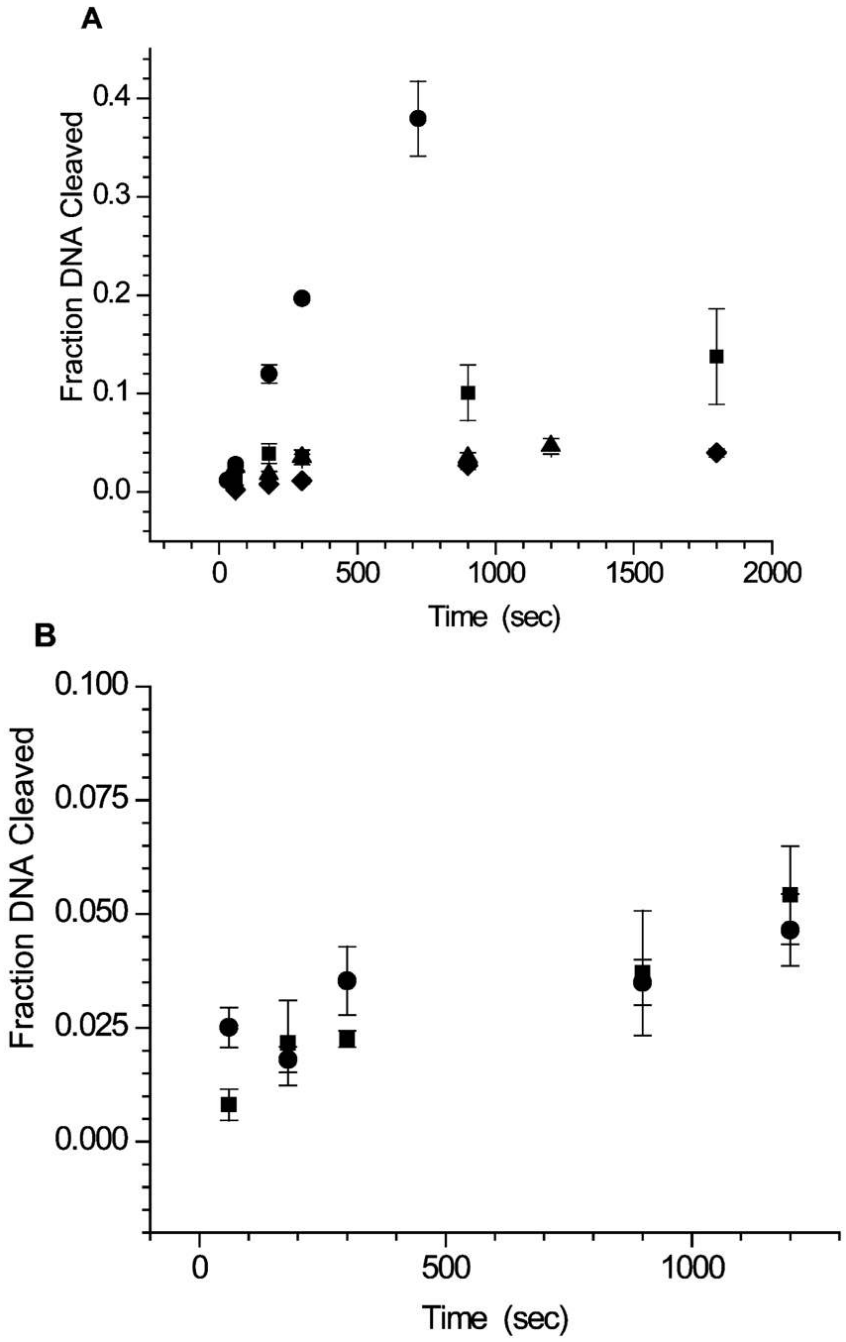

Figure 2.
Excision of thymine glycol (Tg) by Nth as a function of time. (A) Tg (1), circle; LTg (3), triangle; −1 cluster (5), square; +1 cluster (6), diamond. (B) LTg (3), circle; FTg (4), square. Note: [Nth] = 0.25 nM when acting on **1** and 100 nM for reactions with **3**–**6**.

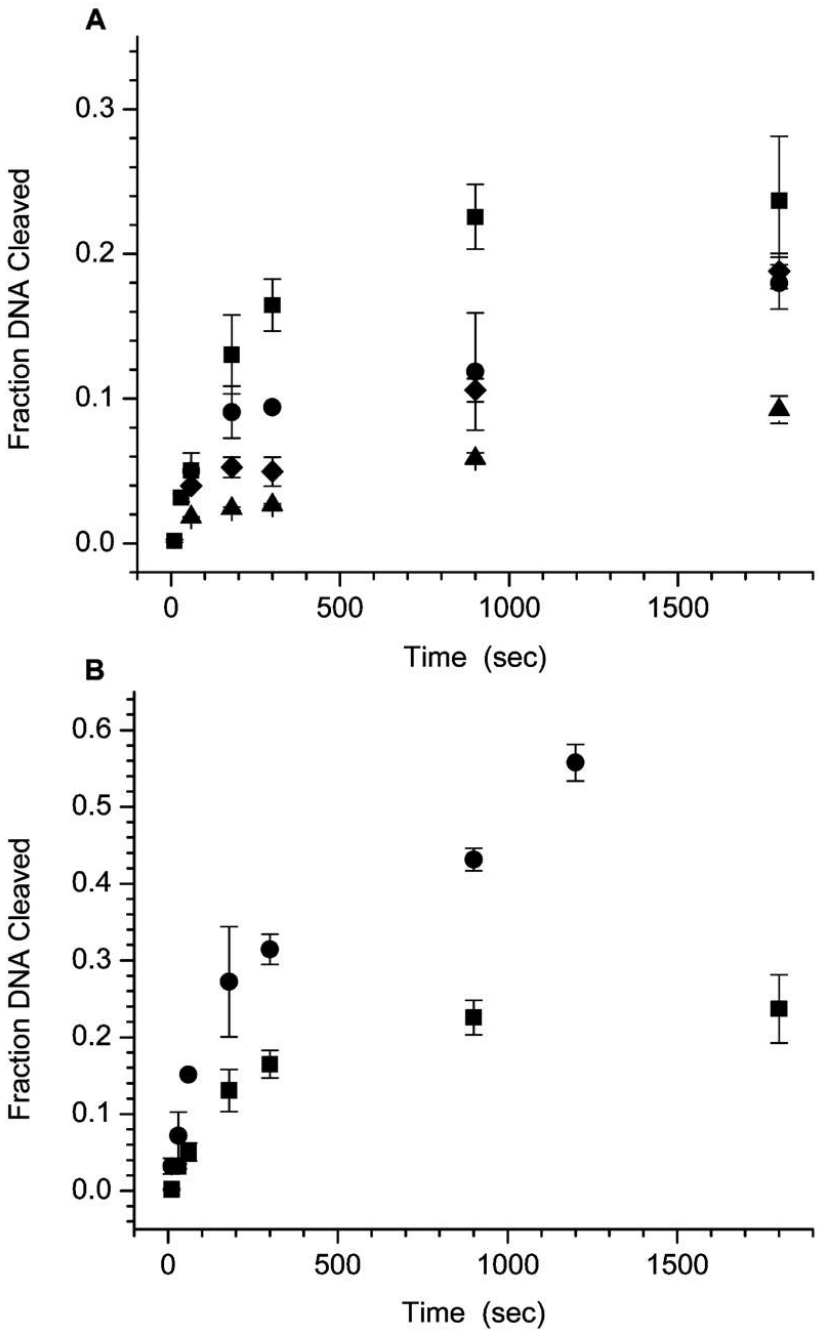

Figure 3.

Incision of 2-deoxyribonolactone (L) or tetrahydrofuran (F) by Nfo as a function of time. (A) L (2), circle; LTg (3), square; −1 cluster (5), triangle; +1 cluster (6), diamond. (B) LTg (3), square; FTg (4), circle. Note: [Nfo] = 5 nM when acting on **2** and 100 nM for reactions with **3**–**6**.

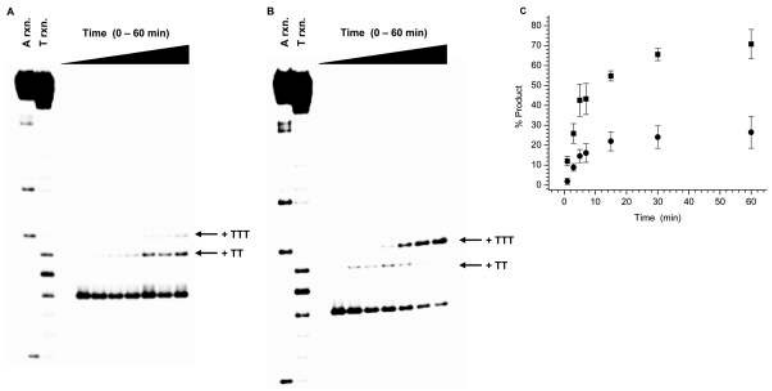

Figure 4.

Strand displacement synthesis on 5′-^{32}P-**8** by Pol β (5 nM). (A) Extension as a function of time in the absence of FEN1. (B) Extension as a function of time in the presence of FEN1 (25 nM). (C) Total product formation as a function of time with FEN1 (square) and without FEN1 (circle). Sequencing reactions selective for T (T rxn) and A (A rxn).

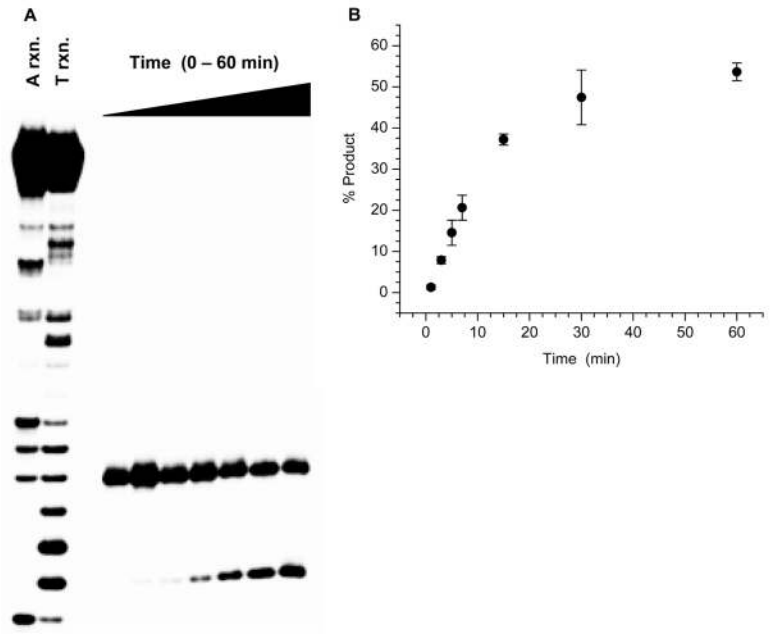

Figure 5.
Cleavage of 3′-^{32}P-**8** by FEN1 (25 nM) as a function of time in the presence of Pol β (5 nM). Sequencing reactions selective for T (T rxn) and A (A rxn).

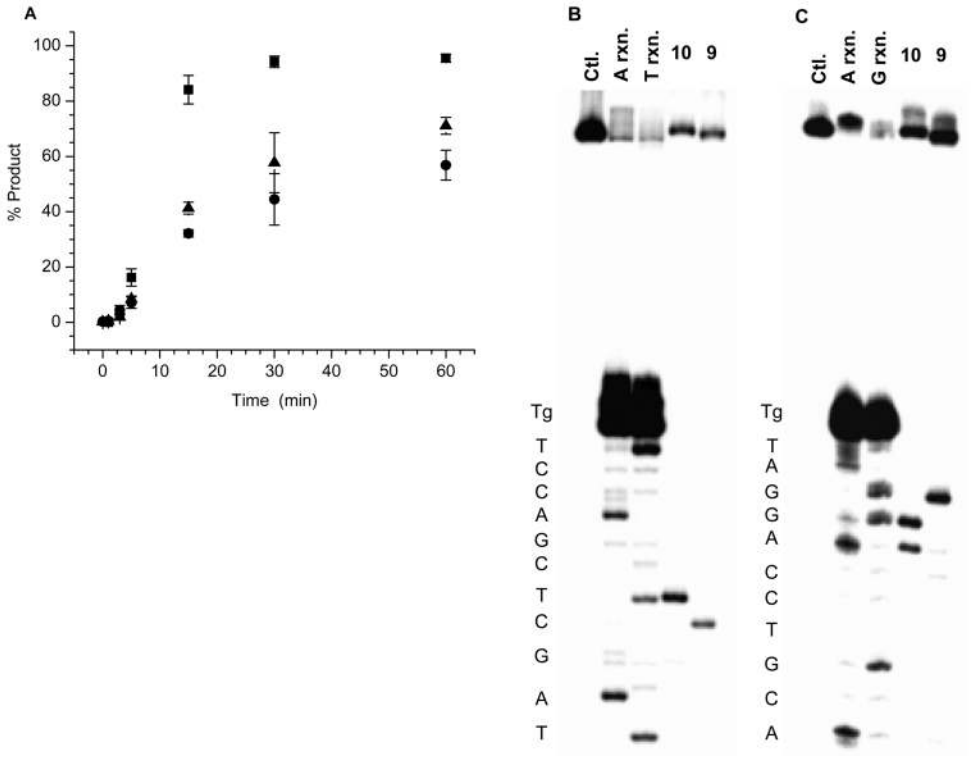

Figure 6.

Incision of FTg tandem lesion (9), Tg (10), and fluoresceinylated standard (Fl, **11**) by UvrABC. (A) Incision in 5′-^{32}P-labeled substrates as a function of time. FTg (9), circle; Tg (10), triangle; Fl (11), square. Autoradiogram indicating the sites of incision in (B)5′-^{32}P-**9** and (C) 3′-^{32}P-**9**. Sequencing reactions selective for T (T rxn) and A (A rxn).

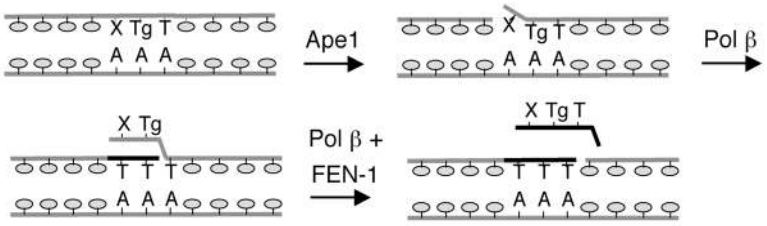

Figure 7.
LP-BER of tandem lesions via strand displacement synthesis. X = L or F.

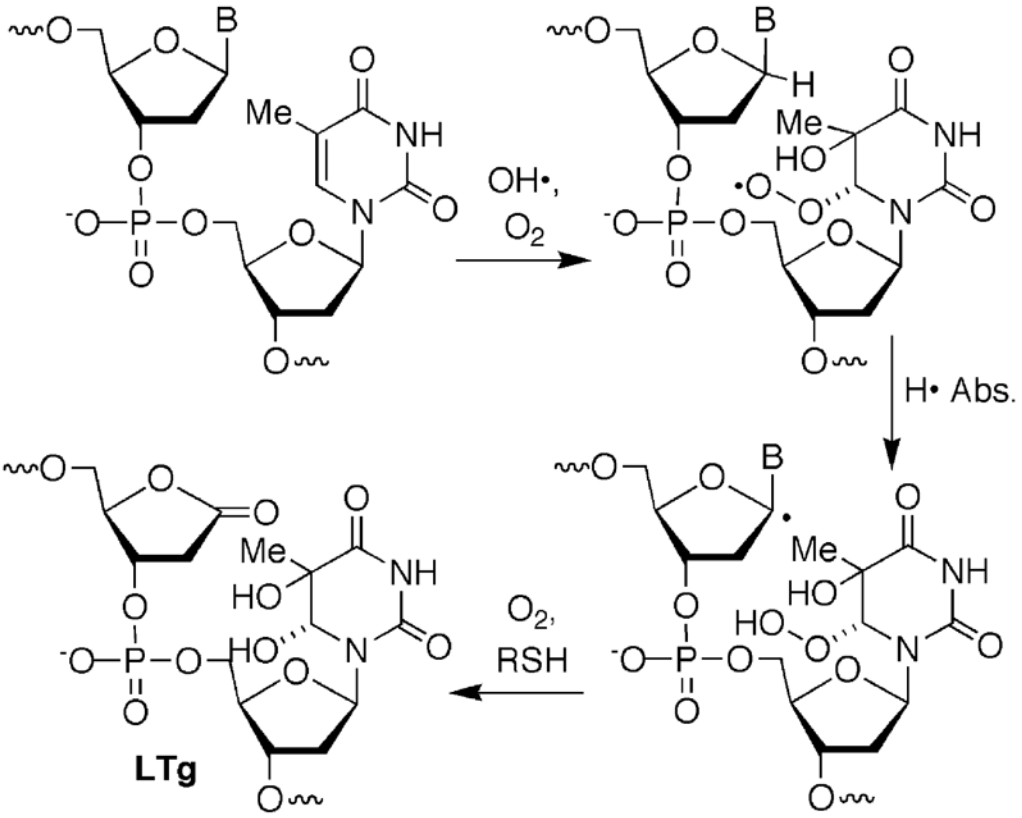

Scheme 1.
Formation of the 5′-LTg Tandem Lesion from a Nucleobase Radical

Table 1

Oligonucleotide Duplexes Used in This Study

5'-d(GAG CTA GCT CGA CC**X** **Y**TA GGA CCT GCA GCT)
3'-d(CTC GAT CGA GCT GGA AAT CCT GGA CGT CGA)

1 **X** = T, **Y** = Tg
2 **X** = L, **Y** = T
3 **X** = L, **Y** = Tg
4 **X** = F, **Y** = Tg

5'-d(GAG CTA GCT CGA CCT **Y**TA GGA CCT GCA GCT)
3'-d(CTC GAT CGA GCT GGA A**X**T CCT GGA CGT CGA)

5 **X** = L, **Y** = Tg

5'-d(GAG CTA GCT CGA CCT **Y**TA GGA CCT GCA GCT)
3'-d(CTC GAT CGA GCT GG**X** AAT CCT GGA CGT CGA)

6 **X** = L, **Y** = Tg

HO OPO_3^{-2}
5'-d(GAG CTA GCT CGA CC **L** **Tg**TA GGA CCT GCA GCT)
3'-d(CTC GAT CGA GCT GG A AT CCT GGA CGT CGA)

7

HO OPO_3^{-2}
5'-d(GAG CTA GCT CGA CC **F** **Tg**TA GGA CCT GCA GCT)
3'-d(CTC GAT CGA GCT GG A AT CCT GGA CGT CGA)

8

5'-d(AGC TAC GTA CGA GCT AGC TCG ACC **XYT** AGG ACC TGC AGC TCC AGA TCT GT)
3'-d(TCG ATG CAT GCT CGA TCG AGC TGG AAA TCC TGG ACG TCG AGG TCT AGA CA)

9 **X** = F, **Y** = Tg
10 **X** = T, **Y** = Tg

5'-d(GAC TAC GTA CTG TTA CGG CTC CAT C**X**C TAC CGC AAT CAG GCC AGA TCT GC)
3'-d(CTG ATG CAT GAC AAT GCC GAG GTA GAG ATG GCG TTA GTC CGG TCT AGA CG)

11 **X** = Fl-dT

Table 2

Steady-State Analysis of Xth Incision

substrate (duplex no.)	K_m (nM)	k_{cat} (min^{-1})	k_{cat}/K_m (nM^{-1} min^{-1})
L (2)[a]	8.3 ± 1.5	171.6 ± 9.3	21.5 ± 4.0
LTg tandem (3)[a]	25.3 ± 3.0	207.7 ± 26.1	7.5 ± 2.5
LTg −1 cluster (5)[b]	14.8 ± 8.0	531.4 ± 117.5	43.1 ± 14.8
LTg +1 cluster (6)[b]	12.7 ± 3.0	713.9 ± 206.0	56.4 ± 12.5

[a] Data are the average ± SD of three experiments.

[b] Data are the average ± SD of four experiments.

Table 3

Steady-State Analysis of APE1 Incision

substrate (duplex no.)	K_m (nM)	k_{cat} (min^{-1})	k_{cat}/K_m (nM^{-1} min^{-1})
L (2)[a]	13.9 ± 1.1	122.1 ± 3.6	8.7 ± 1.6
LTg tandem (3)[b]	12.6 ± 1.4	65.3 ± 15.5	5.2 ± 0.7
FTg tandem (4)[b]	9.3 ± 4.5	18.1 ± 1.3	2.5 ± 1.1
LTg −1 cluster (5)[c]	60.9 ± 17.3	228.1 ± 57.6	4.1 ± 1.4
LTg +1 cluster (6)[a]	37.0 ± 14.0	62.3 ± 7.2	1.9 ± 0.5

[a] Data are the average ± SD of three experiments

[b] Data are the average ± SD of two experiments.

[c] Data are the average ± SD of five experiments.

Table 4

Effects of Tandem and Clustered Lesions on Duplex Melting Temperatures

Duplex	5′-d(GCG GAC CXY TAG GCA G) 3′-d(CGC CTG GAN ATC CGT C) X	Y	N	T_m (°C)	Duplex	5′-d(GCG GAC CTY TAG GCA G 3′-d(CGC CTG GXA ATC CGT C) X	Y	T_m(°C)
12	T	T	A	61. 9 ±0.5	18	Tg	L	47.5 ± 0.6
13	T	Tg	A	51. 9 ±0.3	19	L	Tg	49.3 ± 0.2
14	L	T	A	51.0 ±0.7				
15	L	Tg	A	51. 3 ±0.8				
16	T	T	C	47.1 ±0.1				
17	L	Tg	C	45.9 ±0.1				